Journal of Innovative Optical Health Sciences
Vol. 5, No. 4 (2012) 1250024 (6 pages)

DOI: 10.1142/S1793545812500241

POLARIZATION-SENSITIVE OPTICAL COHERENCE TOMOGRAPHY USING A MODIFIED BALANCE DETECTOR

LI-PING YU
Center for Biomedical Engineering
Chang Gung University
Taoyuan 333, Taiwan, China

JIAN-CHEN GUO
Department of Biomedical Imaging and Radiological Science
National Yang Ming University
Taipei 112, Taiwan, China

LI-DEK CHOU and TE-LUN MA
Graduate Institute of Electro-Optical Engineering
Chang Gung University
Taoyuan 333, Taiwan, China

JHENG-SYONG WU
Department of Optics and Photonics
National Central University Jhongli
320, Taiwan, China

JIANN-DER LEE
Department of Electrical Engineering
Chang Gung University
Taoyuan 333, Taiwan, China

CHIEN CHOU*
Graduate Institute of Electro-Optical Engineering
and Center for Biomedical Engineering
Chang Gung University
Taoyuan 333, Taiwan, China
cchou01@gmail.com

Accepted 28 July 2012
Published 9 October 2012

*Corresponding author.

In conventional polarization-sensitive optical coherence tomography (PS-OCT), phase retardation is obtained by the amplitude of P and S polarization only, and the fast axis angle is obtained by the phase difference in P and S polarizations via Hilbert transformation. In this paper, we proposed a modified PS-OCT setup in which the phase retardation and fast axis angle are simply expressed as the function of the amplitude of P and S polarization and their differential signal. Due to the common-path feature between the two channels of P and S polarization, the fluctuation in the measurement of phase retardation and fast axis angle caused by excess noise and phase noise from the laser source can be reduced by the differential signal of P and S polarization via a modified balance detector. Thus, the signal of phase retardation and fast angle axis in the deep layer of a porcine sample can be improved.

Keywords: PS-OCT; modified balanced detector; Hilbert transformation.

1. Introduction

Linear birefringence is one of the optical properties of an anisotropic medium, which causes different phase velocities to P and S polarized light when propagating in the medium. The phase retardation δ between P and S polarized light and the fast axis angle φ are defined as the linear birefringence parameters of an anisotropic medium.[1−3] Most biological tissues show anisotropic properties, and their fast axis angles are more randomly distributed, thus the birefringence is highly sensitive to their localized fast axis angles. In order to reduce this effect, the use of circularly polarized light is suggested for sample detection. In conventional polarization-sensitive optical coherence tomography (PS-OCT), δ is obtained by the ratio of the amplitudes of P and S polarization,[2,3] and then φ is determined by the phase difference between P and S polarization via Hilbert transformation.[3] Also, in conventional PS-OCT, two quarter-wave plates (QWPs) are used in the reference and sample arms. A QWP in the reference arm provides equal reference power in two orthogonal polarization states, and another QWP in the sample arm ensures a circularly polarized light incident to the sample. In this paper, we propose a modified PS-OCT in which a differential-phase decoder method[4−7] is used while QWP is not used in either reference or sample arms (see Fig. 1). Thus, the polarization states in the reference and sample arms are both circular, and the symmetry between them is good without using additional QWP. The dispersion effect caused by QWP in the use of low coherence source is also reduced. According to our previous studies on differential-phase detection,[4−8] three independent amplitude signals are generated: P and S polarizations and an additional differential signal obtained by a differential amplifier (DA). Because the two input channels (P and S polarizations) into the DA are common-path in the optical setup, the differential signal is detected like a balanced detector, which is the so-called modified balanced detector. Accordingly, the detection signal is improved by using the modified balanced detector.[4,8−10] In this paper, the performance on measuring δ and φ was tested by a Berek's polarization compensator, and the feasibility of obtaining the tomographic images of δ and φ was shown. In addition, an improved performance on phase retardation signal at deep layer of porcine tendon was also demonstrated.

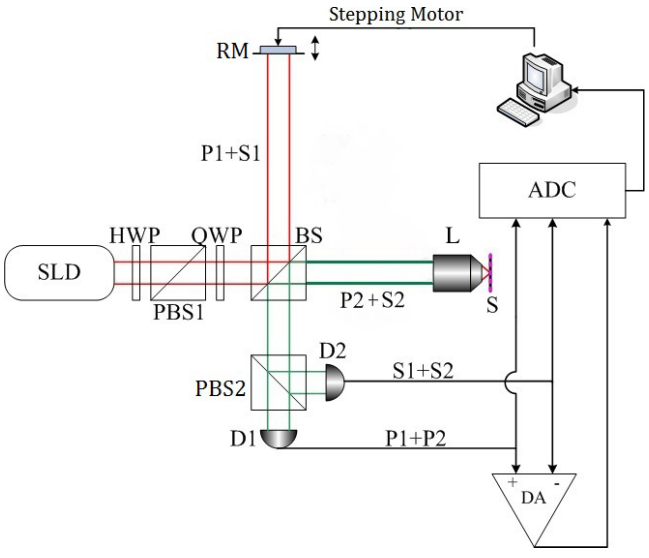

Fig. 1. Experimental setup. SLD, superluminescent diode; HWP, half-wave plate; PBS, polarizing beam splitter; QWP, quarter-wave plate; BS, beam splitter; RM, reference mirror; L, microscope objective (NA = 0.40, 20X); S, sample; D, photo detector; DA, differential amplifier.

2. Method

The modified PS-OCT setup is shown in Fig. 1. It consists of a low coherence source, superluminescent diode (BWC-SLD11, B&W) output collimated beam (the output power is 1.1 mW) with the center wavelength $\lambda_0 = 830\,\text{nm}$ and a bandwidth of $\Delta\lambda = 25\,\text{nm}$. After passing through a half-wave plate (HWP), polarizing beam splitter (PBS1) and a quarter-wave plate (QWP), in which the fast axis is oriented at 45° to the horizontal, a circularly polarized light is output and equally split into a reference and a sample beams by a nonpolarizing beam splitter (BS). After reflection at the sample, the backpropagating light is in an elliptical polarization state, including information on the phase retardation between P and S polarization state and the fast axis angle of the sample. After recombination with the reference beam at the BS, both the sample beam components (P2 + S2) and reference beam components (P1 + S1) are split by a PBS2 forward to P-polarized (P1 + P2) and S-polarized detection channels (S1 + S2). In addition, the differential signal between P and S channels is obtained by a DA (Model DA1855A, LeCory) in the same time, in which the phase difference between reference and sample are reflected on the amplitude of the differential signal. In this setup, the HWP, PBS1 and QWP also play as an optical isolator module to prevent the laser from damage. In order to axially scan the sample, the reference mirror (RM) controlled by a stepping motor (a step resolution is 0.1 μm) is translated along z-axis at a constant speed of 1 mm/s, which is able to provide a stable Doppler frequency shift at 2.4096 kHz. According to the modified PS-OCT setup, the electric field of the reflection beam in reference arm would be:

$$E_R = \left(\frac{R_m}{2}\right)^{1/2} E_0 \begin{pmatrix} 1 \\ i \end{pmatrix} \exp(-i2kl_r), \qquad (1)$$

which is a circularly polarized light. Here R_m is the intensity reflectivity from RM, E_0 is the amplitude of the electric field, k is the wave number and l_r is the optical path length between BS and RM. Meanwhile, the reflection beam after the sample, the electric field at BS is:

$$E_S = J_s J_s \left[\frac{R_s(d)}{2}\right]^{1/2} E_0 \begin{pmatrix} 1 \\ i \end{pmatrix} \exp(-i2kl_s), \qquad (2)$$

which describes a circularly polarized light that is backscattering upon an anisotropic medium. In the above equation, $R_s(d)$ is the intensity reflectivity from the sample at depth d, l_s is the optical path length between BS and sample surface and J_s is the well-known Jones matrix of an anisotropic sample.[11] After recombination of the reference and sample beam with respective to Eqs. (1) and (2), the output amplitudes of heterodyne signals in P and S channels are:

$$|I_P| = \gamma P_0 [R_m R_s(d)]^{1/2} \exp\left\{-\left[\frac{2\Delta l(\ln 2)^{1/2}}{l_\omega}\right]^2\right\} \times [1 - \sin(2\delta)\sin(2\varphi)]^{1/2}, \qquad (3)$$

$$|I_S| = \gamma P_0 [R_m R_s(d)]^{1/2} \exp\left\{-\left[\frac{2\Delta l(\ln 2)^{1/2}}{l_\omega}\right]^2\right\} \times [1 + \sin(2\delta)\sin(2\varphi)]^{1/2}, \qquad (4)$$

respectively. Here, γ is quantum efficiency of photo detectors; P_0 is the initial power which is proportional to $|E_0|^2$; $\Delta l = l_s - l_r$ is the path length difference between sample and reference arms, and l_ω is the coherence length of the low coherence source; δ and φ are the phase retardation and fast axis angle to the anisotropic medium. In addition, the output amplitude of their differential signal from DA is:

$$\begin{aligned} |\Delta I| &= |I_P - I_S| \\ &= 2\gamma P_0 [R_m R_s(d)]^{1/2} \\ &\quad \times \exp\left\{-\left[\frac{2\Delta l(\ln 2)^{1/2}}{l_\omega}\right]^2\right\} \sin(\delta). \end{aligned} \qquad (5)$$

The reflectivity of total intensity R and phase retardation δ can be extracted from Eqs. (3)−(5)

$$R \propto |I_P|^2 + |I_S|^2, \qquad (6)$$

$$\delta = \sin^{-1}\left\{\frac{|\Delta I|}{[2(|I_P|^2 + |I_S|^2)]^{1/2}}\right\}. \qquad (7)$$

δ is directly dependent of ΔI and R. Another relation obtained from Eqs. (3) and (4) is

$$\sin(2\varphi)\sin(2\delta) = (|I_S|^2 - |I_P|^2)/(|I_P|^2 + |I_S|^2). \qquad (8)$$

After we combined Eqs. (7) and (8), the fast axis angle φ can be also determined by I_P, I_S and ΔI

$$\varphi = \frac{1}{2}\sin^{-1}\left\{\frac{|I_S|^2 - |I_P|^2}{|\Delta I|[2(|I_P|^2 + |I_S|^2) - |\Delta I|^2]^{1/2}}\right\}. \qquad (9)$$

According to Eqs. (7) and (9), the expected dynamic range of δ and φ are $0° \leq \delta \leq 90°$ and $-45° \leq \varphi \leq 45°$, respectively. However, the dynamical range of φ becomes half in comparison with conventional PS-OCT.

3. Results

Figure 2 shows the stability of the measured δ within 4 min, when the sampling frequency is 10 Hz. The extra δ was produced by using a Berek's polarization compensator (New Focus, Model 5540) in the sample arm. This compensator allows a variable δ at fixed φ in a wide range of wavelengths. The standard deviation in the measurement is 0.35°, which shows good stability of measuring δ.

Moreover, the system's performance was tested by Berek's polarization compensator while δ and φ can be changed independently. The results were shown in Fig. 3(a), in which the δ of the Berek's polarization compensator was manually varied from 0° to 180° in step of 15° and its φ was held at fixed value of 0°. The dot points indicate that the measurement of δ which are in good agreement with expected curve (solid line). The mean absolute deviation of δ in Fig. 3(a) is $\sim$2.9° to all data points. Figure 3(b) shows the measurements of φ when the φ of Berek's polarization compensator was manually varied from $-45°$ to 45° by a step of 5° whereas the δ was set at 90° during the measurement. However, the mean absolute deviation between given and measured φ is $\sim$8.6°, which was caused by the reasons of imperfect polarization optics and inaccurate calibration of the compensator from the manufacture.[3] Our measurement results are similar to the previous results by using conventional PS-OCT.[3]

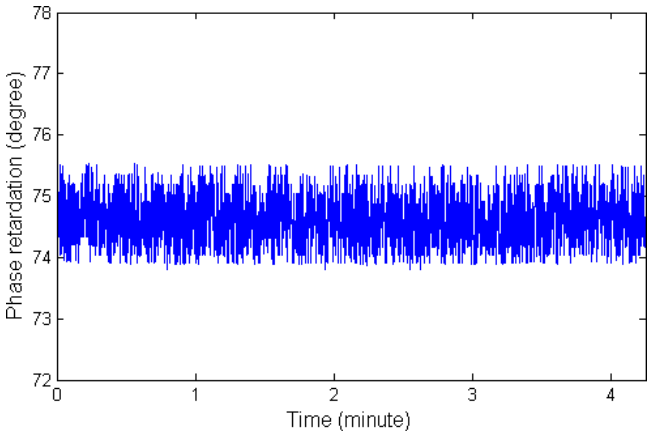

Fig. 2. The stability of phase retardation.

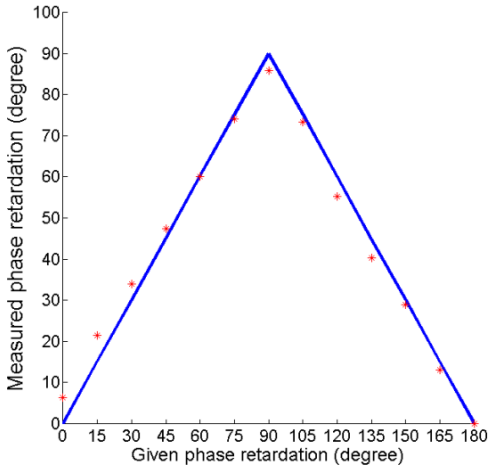

(a)

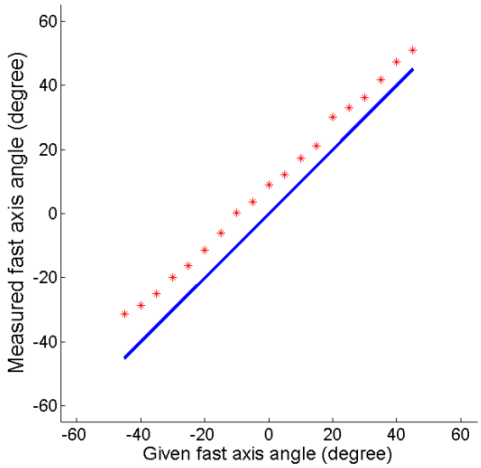

(b)

Fig. 3. Measurement of the change of the phase retardation (a) and fast axis angle (b) by the Berek's polarization compensator. The solid lines present the expected curves.

In order to validate the feasibility of the modified PS-OCT, a porcine tendon was measured. Figure 4 show the tomographic images of (a) the normalized intensity reflectivity, (b) phase retardation δ (in degree), and (c) fast axis angle φ (in degree). The images of the phase retardation and fast axis angle clearly show the structure of collagen fiber in porcine tendon from the surface to 450 μm in depth. Furthermore, in order to demonstrate the ability of reducing phase noise in modified PS-OCT, the conventional PS-OCT was also setup in this experiment.[3] It is noted that only two channels (P and S channels) were obtained by the conventional PS-OCT, and the δ value were obtained only by the amplitude of P and S channels. Figure 5 shows the

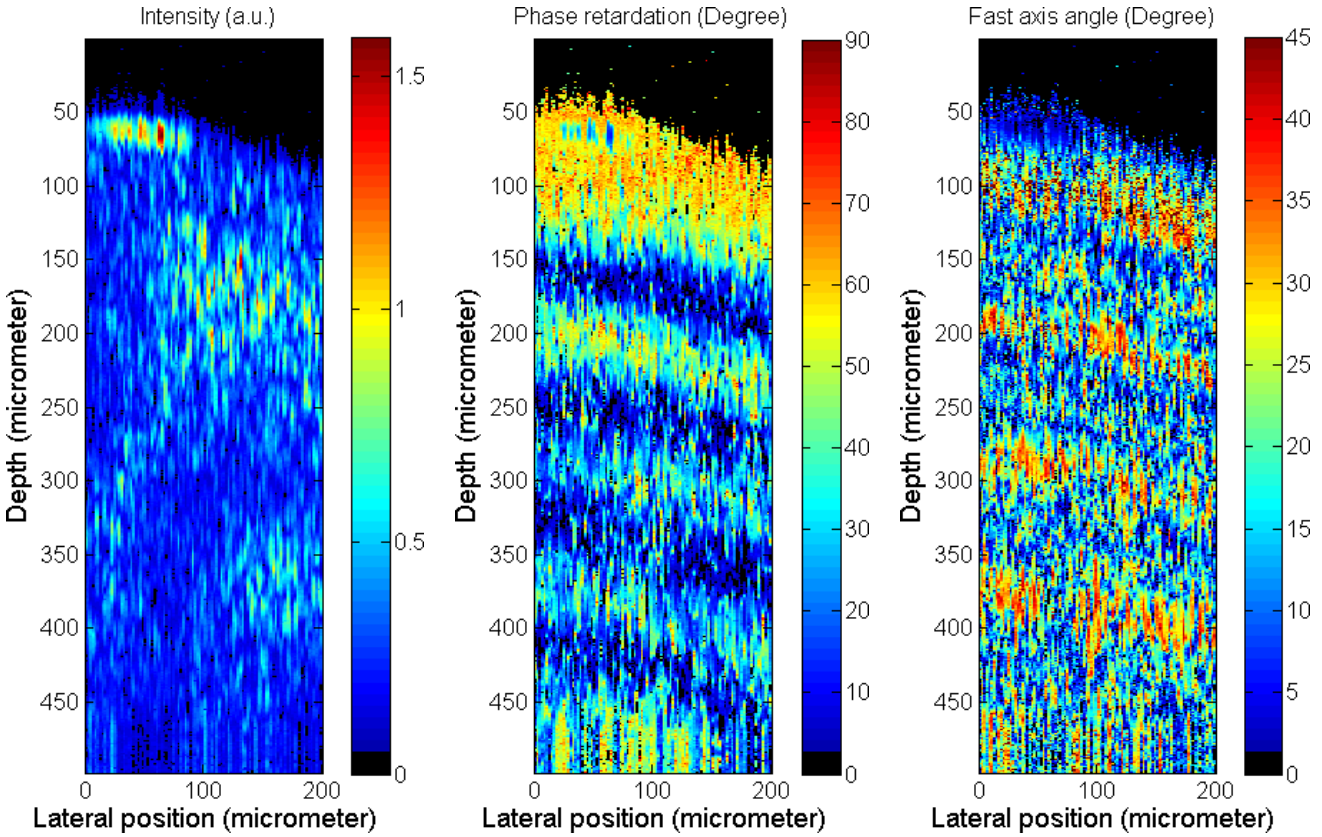

Fig. 4. The tomographic image of a porcine tendon sample shown in: (a) Intensity reflectivity; (b) Phase retardation; (c) Fast axis angle.

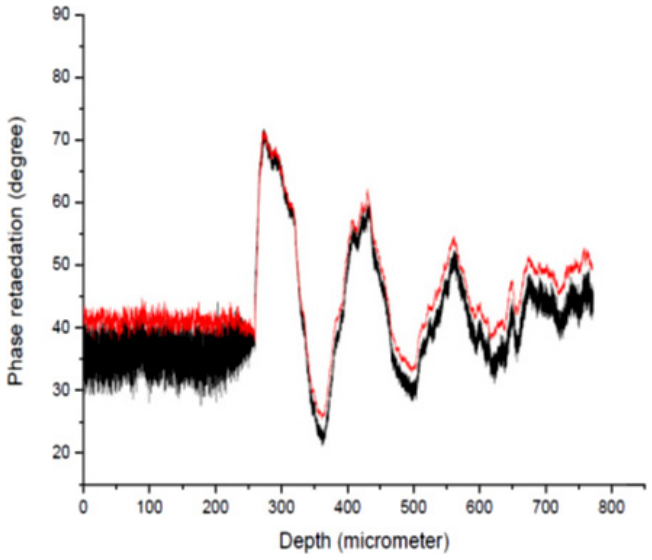

Fig. 5. The phase retardation profile along the optical axis in the measurement of a porcine tendon sample. The PS-OCT with modified balance detector (red line) and the conventional PS-OCT (black line).

change and fluctuation of δ along the depth of a porcine tendon by using conventional PS-OCT (black solid line) and the modified PS-OCT (red solid line), respectively. The profiles along the depth of the sample clearly show less fluctuation in the measurement of phase retardation in modified PS-OCT than that in conventional one. The modified PS-OCT using three polarization output channels simultaneously to obtain δ indeed shows an improvement on measurement of δ at deep layer where a low signal level was resulted.

4. Discussion and Conclusion

A modified PS-OCT which simultaneously outputs three channels of the P and S polarizations and their difference signal was proposed. According to Eqs. (7) and (9), the phase retardation δ and fast axis angle φ can be directly obtained by the three output amplitudes of heterodyne signals. The system performance

on the measurement of δ and φ was also validated by Berek's polarization compensator and the measured values of δ and φ in Fig. 3 are in good agreement with expected values. However, the dynamic range of φ in the conventional setup is twice larger than that in the modified PS-OCT theoretically. In the output channel of ΔI, the excess noise and phase noise are reduced by using the DA, which belongs to a modified balanced detector and in conjunction with the common-path configuration of P and S channels. As results, δ and φ which are dependent on $|\Delta I|$ can be obtained with high signal-to-noise ratio. In addition, a good stability of δ (0.35° in standard deviation within 4 min of repeated measurements) was demonstrated in Fig. 2, while δ at deep layer of showing less fluctuation than conventional PS-OCT was also demonstrated in Fig. 5. It is no doubt that the modified PS-OCT can be extended into frequency domain by using a swept source, and an improvement on phase noise in δ and φ is anticipated as well. Meanwhile, an identical objective in the reference arm is suggestd,[12] which is based on optical symmetry for reducing the wave aberration from low coherence source.

Acknowledgment

This research was partially supported by National Science Council of Taiwan through Grant # NSC95-2221-E-010-015-MY3.

References

1. J. F. de Boer, T. E. Milner, M. J. C. van Gemert, J. S. Nelson, "Two-dimensional birefringence imaging in biological tissue by polarization-sensitive optical coherence tomography," *Opt. Lett.* **22**, 934 (1997).
2. K. Schoenenberger, B. W. Colston, D. J. Maitland, L. B. Da Silva, M. J. Everett, "Mapping of birefringence and thermal damage in tissue by use of polarization-sensitive optical coherence tomography," *Appl. Opt.* **37**, 6026 (1998).
3. C. Hitzenberger, E. Goetzinger, M. Sticker, M. Pircher, A. Fercher, "Measurement and imaging of birefringence and optic axis orientation by phase resolved polarization sensitive optical coherence tomography," *Opt. Express* **9**, 780 (2001).
4. C. Chou, C.-W. Lyu, L.-C. Peng, "Polarized differential-phase laser scanning microscope," *Appl. Opt.* **40**, 95 (2001).
5. C. Chou, H.-K. Teng, C.-C. Tsai, L.-P. Yu, "Balanced detector interferometric ellipsometer," *J. Opt. Soc. Amer. A* **23**, 2871 (2006).
6. C.-C. Tsai, H.-C. Wei, S.-L. Huang, C.-E. Lin, C.-J. Yu, C. Chou, "High speed interferometric ellipsometer," *Opt. Express* **16**, 7778 (2008).
7. C. Chou, H.-K. Teng, C.-C. Tsai, J.-S. Wu, "Differential phase decoder in a polarized optical heterodyne interferometer," *J. Opt. Soc. Amer. A* **25**, 2630 (2008).
8. H.-J. Huang, T.-Y. Hsieh, L.-D. Chou, W.-C. Kuo, C. Chou, "Analog differential-phase detection in optical coherence reflectometer," *Opt. Express* **16**, 12847 (2008).
9. G. P. Agrawal, *Fiber-Optic Communication Systems*, 2nd Edition, Wiley-Interscience, New York (1997).
10. S. Yazdanfar, J. A. Izatt, "Self-referenced Doppler optical coherence tomography," *Opt. Lett.* **27**, 2085 (2002).
11. A. Gerrard, J. M. Burch, *Introduction to Matrix Methods in Optics*, Wiley, New York (1975).
12. W. Drexler, "Ultrahigh-resolution optical coherence tomography," *J. Biomed. Opt.* **9**, 47 (2004).